RNA (2000), *6*:976–987. Cambridge University Press. Printed in the USA.

Cross-talk between orientation-dependent recognition determinants of a complex control RNA element, the enterovirus *ori*R

WILLEM J.G. MELCHERS,[1] JUDITH M.J.E. BAKKERS,[1] HILBERT J. BRUINS SLOT,[2,5] JOEP M.D. GALAMA,[1] VADIM I. AGOL,[3,4] and EVGENY V. PILIPENKO[3,6]

[1]University Medical Center Nijmegen, Department of Medical Microbiology, 6500 HB Nijmegen, The Netherlands
[2]University of Nijmegen, Centre for Molecular and Biomolecular Informatics, 6500 GL Nijmegen, The Netherlands
[3]M.P. Chumakov Institute of Poliomyelitis and Viral Encephalitides, Russian Academy of Medical Sciences, Moscow Region 142782, Russia
[4]Moscow State University, Moscow 119899, Russia

ABSTRACT

The coxsackie B3 virus *ori*R is an element of viral RNA thought to promote the assembly of a ribonucleoprotein complex involved in the initiation of genome replication. The mutual orientation of its two helical domains X and Y is determined by a kissing interaction between the loops of these domains. Here, a genetic approach was worked out to identify spatial orientation-dependent recognition signals in these helices. Spatial orientation changes (due to linear and rotational shifts) were introduced by appropriate insertions/deletions of a single base pair into one or both of the domains, and phenotypic consequences caused by these mutations were studied. The insertion of a base pair into domain Y caused a defect in viral reproduction that could be suppressed by a base-pair insertion into domain X. Similarly, a defect in viral replication caused by a base-pair deletion from domain X could be suppressed by a base-pair deletion from domain Y. Thus, certain areas of the two domains should cross-talk to one another in the sense that a change of space position of one of them required an adequate reply (change of space position) from the other. Phenotypic effects of the local rotation of one or more base pairs (and of some other mutations) in either domain X or domain Y suggested that the two most distal base pairs of these domains served as orientation-dependent recognizable signals. The results were also consistent with the notion that the recognition of the distal base pair of domain Y involved a mechanism similar to the intercalation of an amino acid residue.

Keywords: cross-talk; enterovirus; recognition signals; replication; RNA structure

INTRODUCTION

There is a class of RNA *cis*-acting control elements that are represented by complex multidomain structures, as exemplified by viral and cellular internal ribosomal entry sites (Jackson & Kaminski 1995; Belsham & Sonenberg, 1996; Lemon & Honda, 1997; Stewart & Semler, 1997) and origins of genome replication of some RNA viruses (Giege, 1996; Pilipenko et al., 1996; Melchers et al., 1997; Xiang et al., 1997). Essential parts of these elements may be involved in the specific recognition of ligands (proteins and nucleic acids) or serve to support structural integrity of the whole element. To understand the molecular mechanism of functioning of a given element, the partial functions, if any, of its constituent parts should be defined.

Efficient tools are available to study functional significance of primary, secondary, and tertiary RNA structures, for example, comparative sequence analysis (Pilipenko et al., 1989a, 1989b, 1992b; Gutell et al., 1994; Kolykhalov et al., 1996; Luck et al., 1996; Springer & Douzery, 1996; Hofacker et al., 1998; Le et al., 1998; Massire et al., 1998), site-directed mutagenesis (Lee et al., 1997; Ishii et al., 1999; Kieft et al., 1999; Rust et al., 1999), domain shuffling (Frolov et al., 1998; Smalle et al., 1998; Gromeier et al., 1999), (pseudo)revertant analysis (Pilipenko et al., 1992a, 1995; Hoffman & Palmenberg, 1996; Klovins et al., 1998; Stewart & Semler, 1998), and others. Current research is largely focused on the

Reprint requests to: Willem J.G. Melchers, University Medical Center Nijmegen, Department of Medical Microbiology, P.O. Box 9101, 6500 HB Nijmegen, The Netherlands; e-mail: w.melchers@mmb.azn.nl.
[5]Present address: Unilever Research Laboratory, P.O. Box 114, 3130 AC Vlaardingen, The Netherlands.
[6]Present address: Department of Neurology, University of Chicago, Chicago, Illinois 60637, USA.

elucidation of the role of specific nucleotides or nucleotide motifs (Uhlenbeck et al., 1997; Robertson et al., 1999); secondary structure elements like hairpins, bulges, and other distortions of the canonical pairing in double-stranded helices (Holbrook et al., 1991; Baeyens et al., 1996; Fourmy et al., 1996; Jang et al., 1998; Wu & Tinoco, 1998); and tertiary interactions of the pseudoknot, kissing and other types (Pilipenko et al., 1996; Deiman & Pleij 1997; Melchers et al., 1997; Hilbers et al., 1998; Kolk et al., 1998; Kieft et al., 1999; Tinoco & Bustamante, 1999). There are, however, features of complex RNA elements that until now attracted less attention, perhaps because of the lack of adequate approaches to investigate their significance. In particular, the mutual orientation of helical elements in complex multidomain RNA structures should be mentioned in this regard.

The goal of the present study was to develop an approach to study this problem, using the enterovirus RNA *cis*-element *ori*R as a well-characterized model system (Fig. 1). The enteroviral *ori*R is a *cis*-acting element located in the 3′ untranslated region of viral RNA and is thought to be involved in the initiation of the complementary (negative) strand (Pilipenko et al., 1996; Melchers et al., 1997). It is known to contain stem-loop structures, domains X and Y, and, in some enteroviruses, domain Z, as well as a portion of the genetically encoded poly(A) tract. Domain Z is stacked to domain Y, generating a coaxial helical element (Melchers et al., 1997). We have recently shown that a sequence within the loop of domain X pairs with a complementary sequence in the loop of domain Y to form a tertiary intramolecular "kissing" (K) domain (Pilipenko et al., 1996; Melchers et al., 1997; Wang et al., 1999). This domain could be stacked to the X domain to form a second coaxial helix, which is connected to the Y domain by a single-stranded, highly conserved nucleotide stretch. The lengths of the helical domains X and Y are highly conserved. Their mutual orientation is largely determined by the structure of the K domain, which appears to be quite stable, as suggested by molecular dynamics calculations (Wang et al., 1999; H.J. Bruins Slot, E.V. Pilipenko, V.I. Agol & W.J.G. Melchers, unpubl.).

The experiments described here were aimed at elucidating the biological significance of the mutual orientation of the X and Y domains. It was found that, to ensure proper *ori*R function, certain areas of the two helical domains should cross-talk to one another in the sense that a change of a spatial position of one of them required an adequate change of the relative position of the other. The areas possibly involved in the cross-talk were characterized.

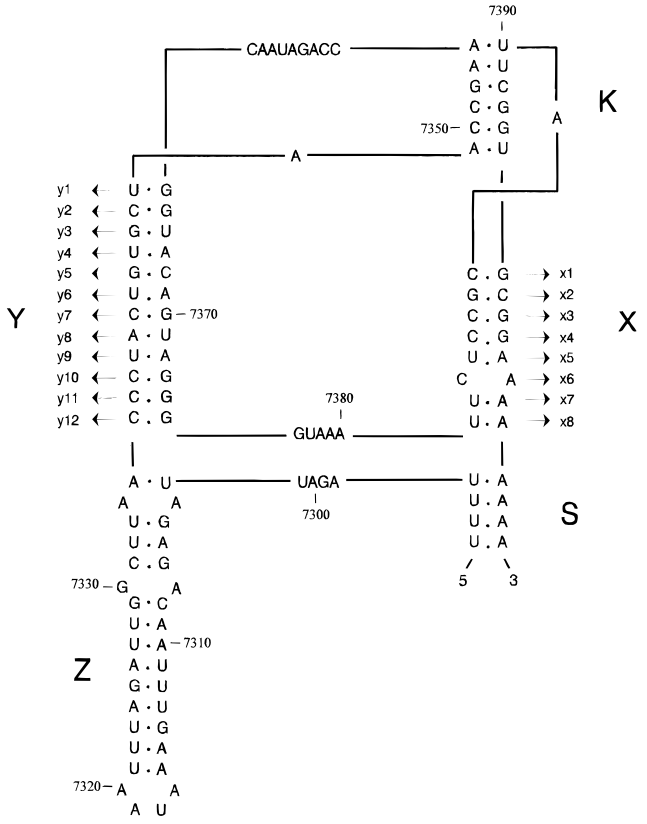

FIGURE 1. Tertiary structure of the coxsackievirus *ori*R. The *ori*R is formed by two coaxial elements consisting of the stacked helical domains Y-Z and K-X-S. The elements are interconnected by the single-stranded stretches $_{7376}$GUAAA$_{7380}$ and $_{7298}$AGAU$_{7301}$. The top-to-bottom base pairs in domains Y and X are indicated as y1–y12 and x1–x8, respectively.

RESULTS

The rationale

The enteroviral *ori*R (Fig. 1) is largely composed of two helices "cemented" by the kissing interaction. In the coxsackieviruses each of the helices in turn consists of coaxially stacked elements, Y and Z on the one hand and K, X, and S on the other. Among sequenced enterovirus RNAs the X and Y domains are well conserved in sequence and in length, always containing 8 and 12 bp, respectively. The *ori*R structure appears to be relatively rigid due to the kissing interaction. It is very likely that the major function of the *ori*R consists of promoting the assembly of a multi-component ribonucleoprotein complex ensuring efficient protein-primed initiation of negative RNA strand synthesis (Todd et al., 1995; Mellits et al., 1998; reviewed in Agol et al. 1999). The assembly obviously requires multiple RNA–protein and protein–protein interactions and should be subjected to certain spatial constraints.

To evaluate the significance of the mutual orientation of the X and Y domains, the following approach was developed. A base pair was inserted into, or deleted from, the helical moieties of either of these domains. In addition to the corresponding length change, this mutation should also cause a rotational shift of about 33°

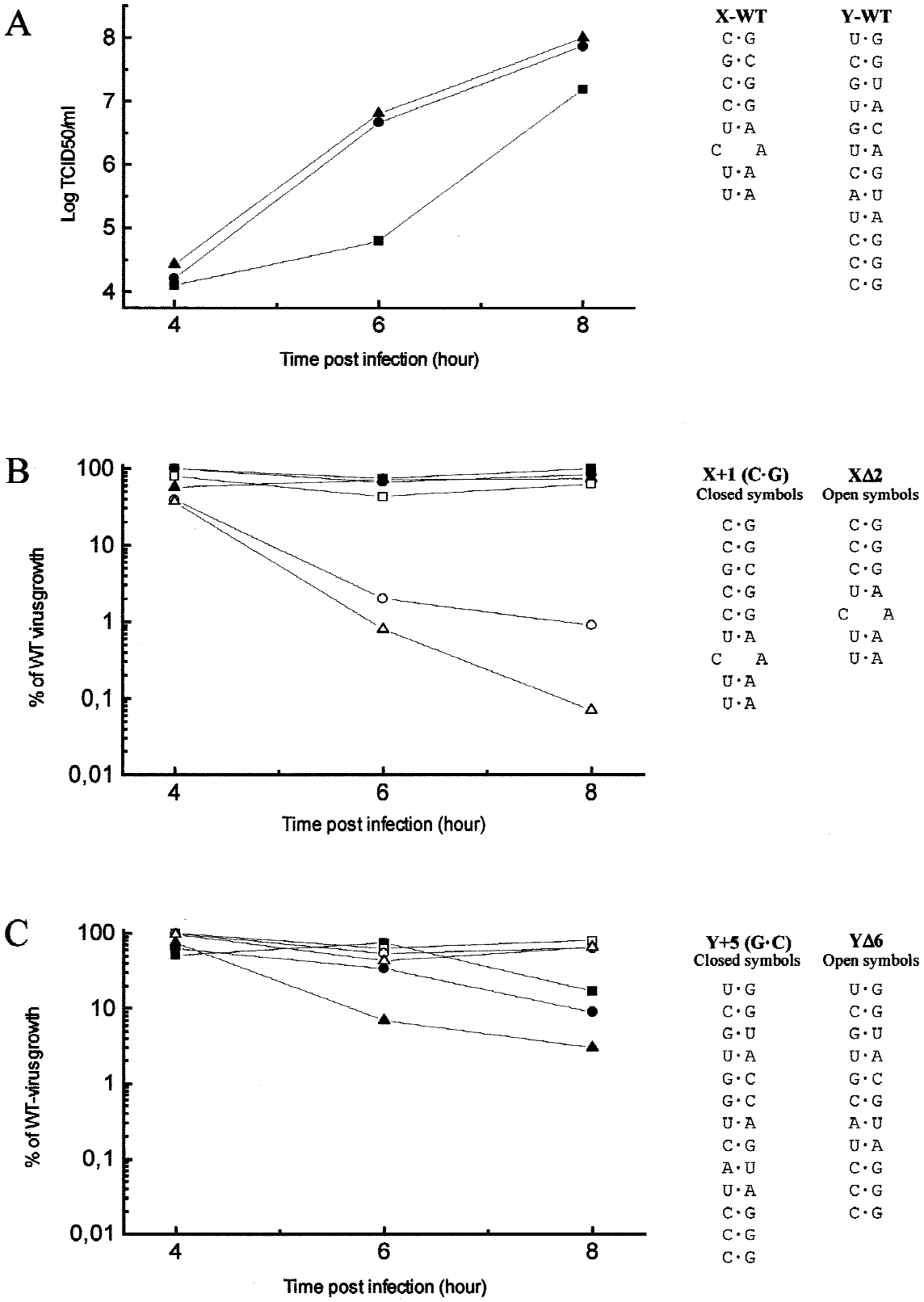

FIGURE 2. Single-cycle growth curves of the mutant viruses. Vero cells were infected with wild-type and mutant viruses at a MOI of 1TCID$_{50}$ per cell. The cells were grown at 33, 36, and 39 °C for 4, 6, and 8 h. Virus titers were determined as described in Materials and methods. The different mutants and the mutant genotypes are indicated in the figure and described in detail in the text. The growth curves at 33 °C are represented by square symbols, at 36 °C by circles and at 39 °C by triangles. (*Figure continues on facing page.*)

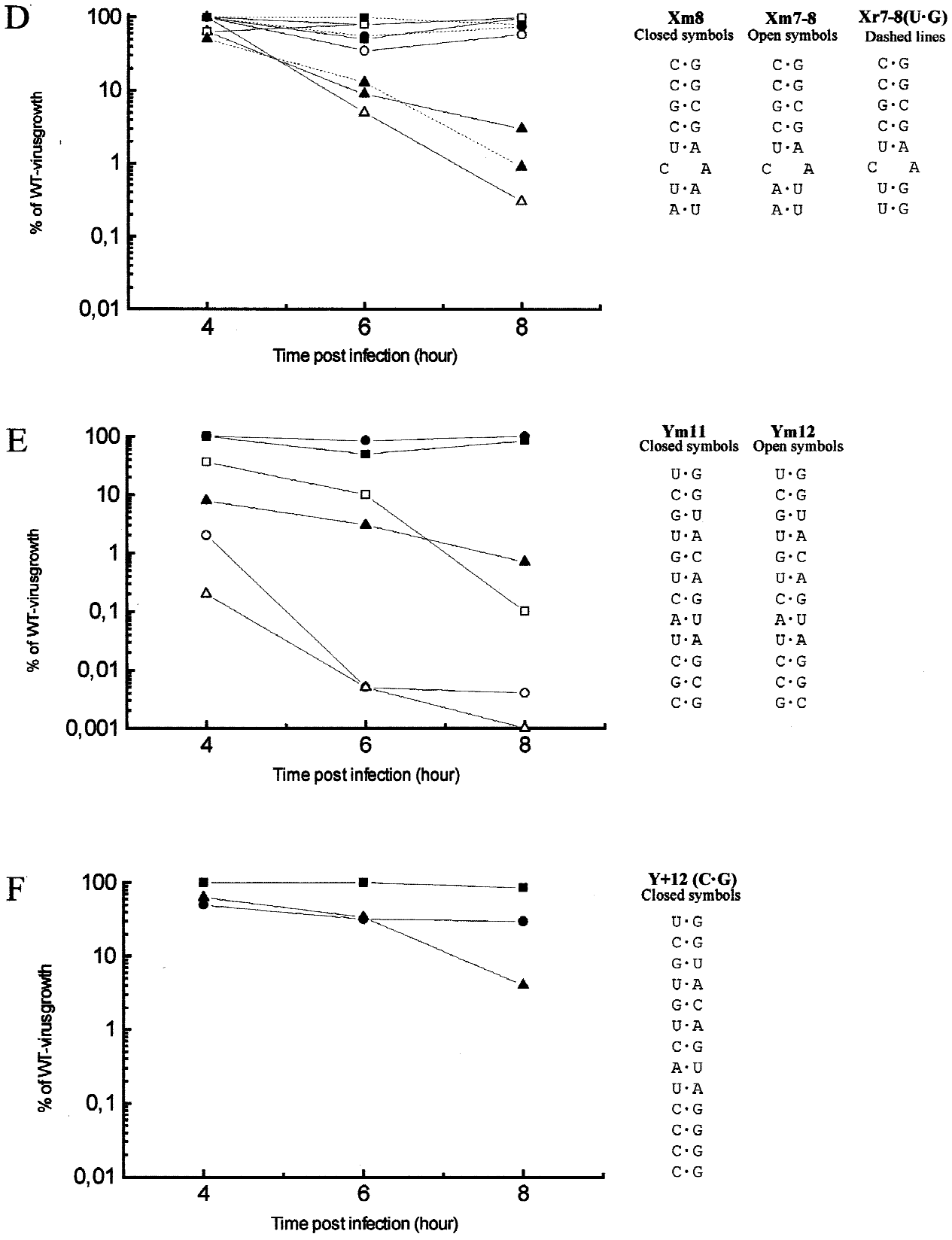

FIGURE 2. *Continued.*

of the K-distal portion of the helix relative to its proximal part, as well as a change in the spatial relationship between the rotated portion of the mutated helix and other areas of the *ori*R. If such a (presumably) bulky ligand as the initiating RNP should simultaneously recognize specific signals on the two helical elements, rotation of one of them may adversely affect the efficient ligand binding and hence also the viral replication. However, it could be assumed that certain alterations of the space position of the second helix may restore optional mutual orientation of the recognizable signals. If this is the case, then these orientation-dependent signals could be mapped by studying phenotypic manifestations of changes in the relative spatial positions of short segments of the helix. Such local alteration could be achieved by either "bracketing" of the target element by a base-pair insertion and a base-pair deletion (the bracketed region and the distal part of the helix relative to the kissing domain will be rotated by 33° along with a linear shift of 3.2 Å) or by mirroring of one or more base pairs.

On the basis of the above considerations, appropriate mutations were engineered into the *ori*R of coxsackie B3 virus. Obviously, the loss/acquisition of a base pair should also bring about primary structure changes. To minimize possible phenotypic consequences of this, the mutations were engineered into loci of the helical elements known or presumed to be tolerant to the alterations in the nucleotide sequence (Fig. 1). The distal 6 bp of domain Y ($_{7336}$CCCUAC$_{7341}$/$_{7370}$GUAGGG$_{7375}$) are highly conserved among different enteroviruses (Pilipenko et al., 1992b; Wang et al., 1999). Also, either disturbing the complementarity or mirroring of the 4 distal bp of the enteroviral Y domain resulted in dead phenotypes, indicating that the nucleotide sequence as such might be important for its function (Pierangeli et al., 1995). Although the sequence of the K domain–proximal 5 bp of the Y domain ($_{7343}$GUGCU$_{7347}$/$_{7364}$GGUAC$_{7368}$) does not seem to be of importance (Melchers et al., 1997), it has been suggested that they are part of a pseudoknot structure (Jacobson et al., 1993). Taking into account these facts, the base-pair insertions/deletions in the Y domain were targeted to, or adjacent to, base pair U$_{7342}$-A$_{7369}$. Specifically, a G•C insertion was introduced between U$_{7342}$•A$_{7369}$ and G$_{7343}$•C$_{7368}$ base pairs [Y+5(G•C)] thereby increasing the length of the Y domain and rotating the distal part of the helix relative to its proximal portion by ~33° clockwise. In another construct [YΔ6], the U$_{7342}$•A$_{7369}$ base pair was deleted, shortening the Y stem and rotating its distal part by ~33° counterclockwise.

The distal base pairs of domain X ($_{7381}$UU$_{7382}$/$_{7402}$AA$_{7403}$) are also very well conserved among the different enteroviruses (Pilipenko et al., 1992b; Wang et al., 1999). Although no data are available concerning the mispair C$_{7383}$-A$_{7401}$, it is highly conserved among the coxsackie B-like viruses and may constitute an important functional feature, as was shown in other cases (Hellendoorn et al., 1997). To keep this structural feature intact, the base-pair insertion/deletions were introduced into the proximal part of the X stem. Thus in X+1(C•G), a C•G base pair was inserted between the G$_{7387}$•C$_{7397}$ and C$_{7388}$•G$_{7396}$ pairs, extending the X helix and simultaneously rotating its distal portion ~33° clockwise. In another construct, XΔ2, the G$_{7387}$•C$_{7397}$ pair was deleted, shortening the stem and rotating it approximately 33° counterclockwise.

The design of constructs used to locate recognizable signals will be presented below.

Phenotypic effects of single base-pair insertions/deletions

The effect of the *ori*R structural alterations on the viral phenotype was tested by transfecting Vero cells with RNA transcripts of the engineered constructs. A cytopathic effect (CPE) was observed upon transfection of all of the RNAs with the single base-pair insertions/deletions described in the preceding section. The growth characteristics of the viruses obtained were further analyzed by single-cycle growth analysis at 33, 36, and 39 °C (Fig. 2; Table 1). The viruses with a single base-pair insertion in the stem of domain X [X+1(C•G)] (Fig. 2B) or a single base-pair deletion from the stem of domain Y [YΔ6] (Fig. 2C) exhibited growth characteristics similar to those of wild-type virus vCB3/T7. On

TABLE 1. Phenotypic expression of mutations in X and Y domains.

Mutant (vCB3-3UTR:)	Percentage of wild-type (WT) virus growth		
	33 °C	36 °C	39 °C
X+1(C•G)	WT	WT	WT
XΔ2	60	<1	<0.1
Y+5(G•C)	50	10	<10
YΔ6	WT	WT	WT
Y+5(G•C)/Δ10	WT	WT	WT
XΔ2/+8(U•A)	WT	WT	WT
X+1(C•G)/Y+5(G•C)	WT	WT	WT
XΔ2/YΔ6	WT	WT	WT
Xm6	WT	WT	WT
Xr6(C•G)	WT	WT	WT
Xm7	WT	WT	WT
Xm8	WT	WT	<10
Xm7–8	WT	WT	<1
Xr7–8(U•G)	WT	WT	<1
Ym7–9	WT	WT	WT
Ym11	WT	WT	<10
Ym12	<0.1	<0.01	<0.01
Y+12(G•C)	—	—	—
Y+12(C•G)	WT	30	<10
YΔ6/+12(C•G)	WT	WT	WT

the other hand, a base-pair deletion from the helix of domain X [XΔ2] resulted in a severe temperature-sensitive phenotype with a virus yield less than 0.1% of that of wild-type at 39 °C (Fig. 2B, Table 1). Similarly, the construct with an insertion in the stem of domain Y [Y+5(G•C)] produced a temperature-sensitive virus, although in this case the temperature dependence was less pronounced (Fig. 2C, Table 1).

Thus, shortening of the X domain and lengthening of the Y domain brought about a temperature-sensitive phenotype, whereas lengthening of the X domain and shortening of the Y domain resulted in no marked phenotypic changes.

The *ori*R overall geometry was not altered by single base-pair insertions/deletions

To evaluate effects of the single base-pair deletions and insertions on the gross arrangement of the *ori*R, the wild-type and mutated RNAs were chemically and enzymatically probed (Fig. 3). The probing patterns for the mutants X+1(C•G), XΔ2, Y+5(G•C), and YΔ6 RNA species did not markedly differ from each other and from that of the wild-type RNA, implying the retention of the major structural features in the engineered RNAs (Fig. 4). It is noteworthy that the $_{7350}$CCG$_{7352}$ stretch in the loop of domain Y appeared to have the same CV1-nuclease generated cleavage sites as in the case of the wild-type RNA, indicating the preservation of the kissing interaction. The stem structure of domain X in mutant XΔ2 appeared to be somewhat less susceptible to the double-strand-specific nuclease, as compared to the wild-type RNA and the other mutated RNAs, most probably due to the stem shortening.

Thus, the single base-pair insertions/deletions in the helices of domain X and Y did not result in any appreciable changes in the overall geometry of the *ori*R.

Changes in mutual orientation of the domains rather than in their length were responsible for the phenotypic effects of single base-pair insertions/deletions

The single base-pair insertions/deletions were accompanied not only by changes in the length of components of the *ori*R but also by modification of their relative spatial positions, caused by rotation of the helix. To discriminate between these two effects, an attempt to suppress the adverse manifestations of the structural alteration of one domain by appropriate modification of the other domain (see The rationale) was undertaken. This attempt proved to be successful.

Indeed, the adverse phenotypic effect of the deletion of base pair G_{7387}•C_{7397} from domain X was completely suppressed by the deletion of base pair U_{7342}•A_{7369} in Y domain (virus XΔ2/YΔ6), whereas the temperature-sensitive phenotype caused by the insertion of a base pair at position 5 of the Y domain was suppressed by a base-pair insertion at position 2 of domain X [virus X+1(C•G)/Y+5(G•C)] (Table 1).

Thus, these results strongly suggested that the lengths of domains X and Y could be altered without pheno-

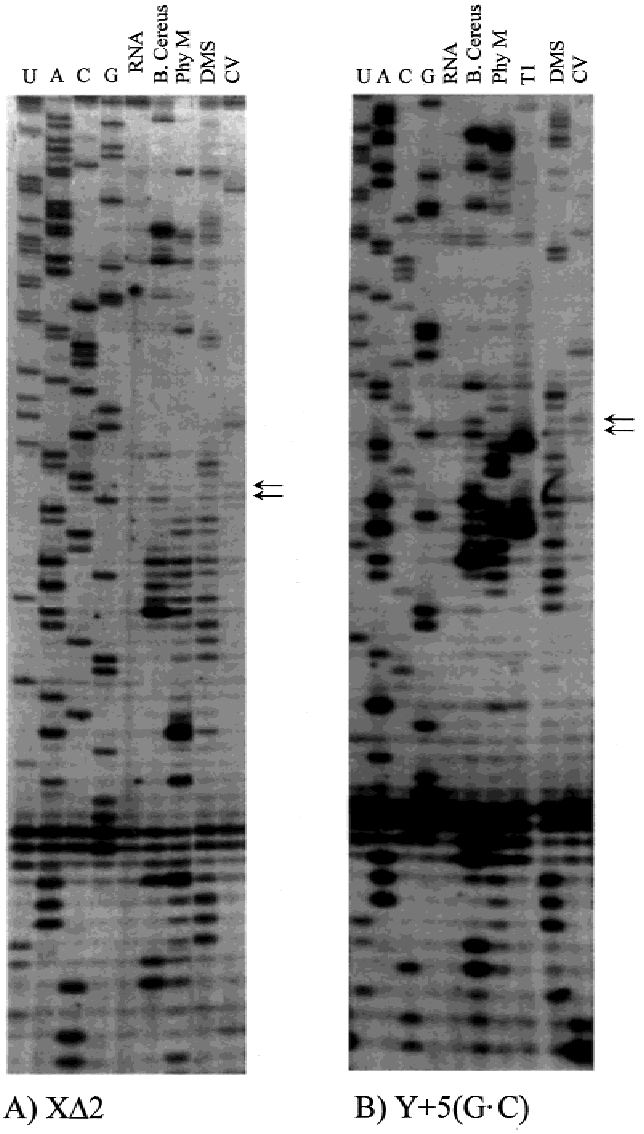

FIGURE 3. Chemical and enzymatic probing of the coxsackie B3 virus *ori*R. The virus RNAs were digested or treated with RNase T1, Phy M, *B. cereus*, DMS, and cobra venom nuclease V1 (CV1), as described in Materials and methods, and then they were used as templates for the oligonucleotide-primed cDNA synthesis by reverse transcriptase. Lane RNA corresponds to nontreated RNA samples. Lanes U, A, C, and G correspond to the samples containing untreated RNA templates and appropriate terminators for DNA synthesis. Shown are the temperature-sensitive mutants XΔ2 (**A**) and Y+5(G•C) (**B**). For XΔ2 the RNase T1 digestion is missing in this figure. Because the primer $(T)_{14}$CCG was used as primer for cDNA synthesis in XΔ2, the base-pair deletion itself cannot be visualized in the figure. However, the $_{7350}$CCG$_{7352}$ stretch in the loop of domain Y appeared to have the same CV1-nuclease generated cleavage sites (see arrows) as in the case of the wild-type RNA (Melchers et al., 1997), indicating the preservation of the kissing interaction in both mutants.

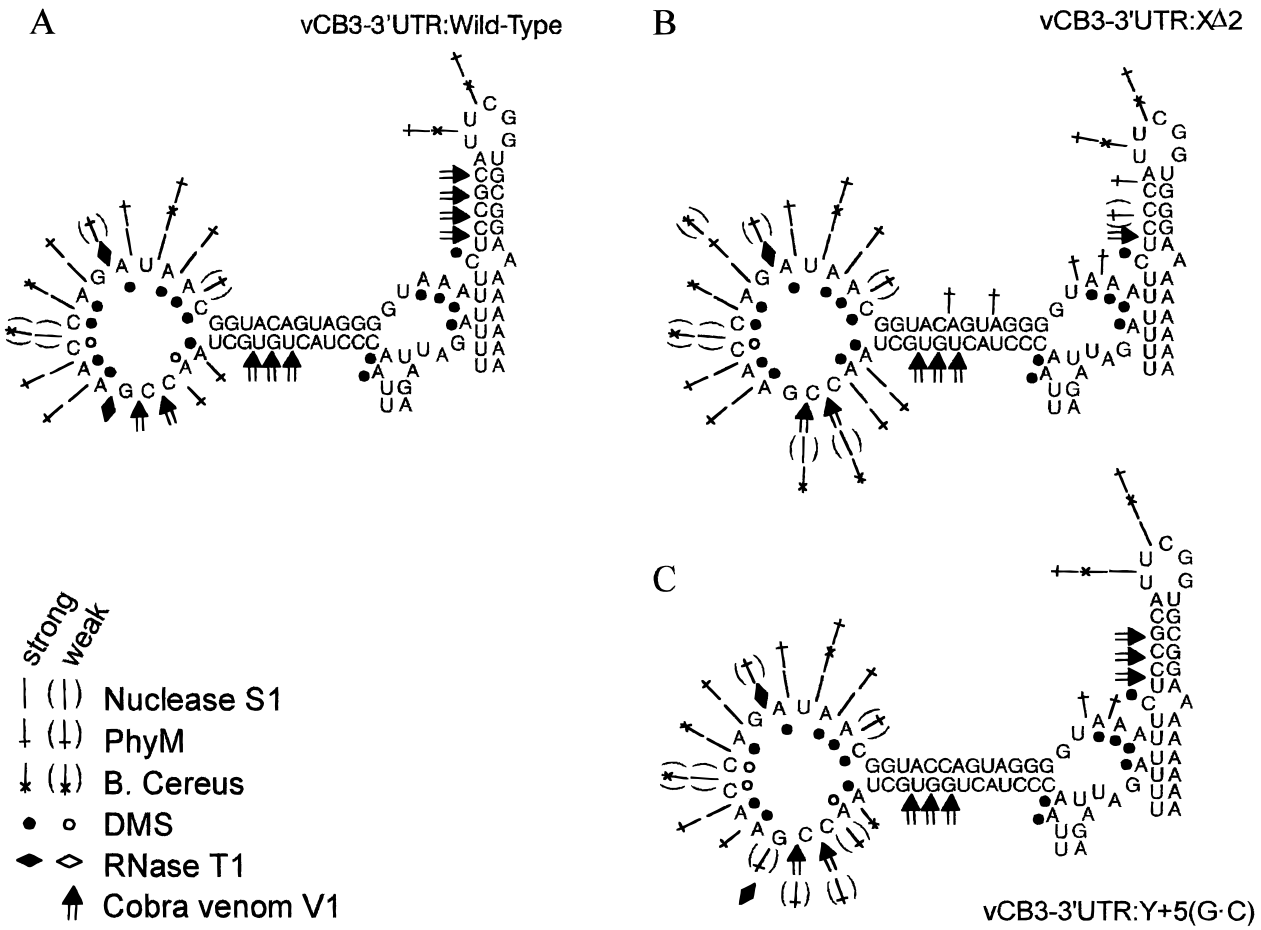

FIGURE 4. Structural probing of the *ori*R. RNA transcripts of the wild-type (**A**) and the temperature-sensitive mutants XΔ2 (**B**) and Y+5(G•C) (**C**) were digested or treated with RNase T1, Phy M, *B. cereus*, DMS, and CV1, and used as templates for oligonucleotide-primed cDNA synthesis. The positions of the cleavages or modifications induced by the relevant probes are indicated. Relatively moderate signals are marked by open and bracketed symbols. For simplicity, the Z-domain was omitted from the figure.

typic modifications provided appropriate changes in their mutual orientation took place. In turn, this could mean that certain areas of the two domains were coordinately involved in the interaction with a common ligand.

Identification of orientation-dependent recognition signals in domain X

To define physiologically important orientation-dependent areas of domain X, an additional set of mutants was designed (see The rationale). The rotation of a significant part of the X domain was not manifested in a phenotypic alteration, as evidenced by the wild-type growth properties of virus XΔ2/+8(U•A) (Table 1). In this virus, a base-pair deletion at position 2 of domain X (which by itself was accompanied by a temperature-sensitive replicative defect) was functionally compensated by a base-pair (U•A) insertion at position 8 of the same domain. It should be noted that the structure of the most distal part of domain X consisting of two U•A pairs was not altered by this mutation. This was an important point because the distal part appeared to carry important *cis*-acting determinants.

Indeed, whereas the A•U-to-U•A mirroring at the penultimate position 7 of domain X (virus Xm7) was phenotypically silent (Table 1), analogous mirroring of the most distal position 8 of this domain rendered the virus (Xm8) thermosensitive (Fig. 2D). Even a greater level of thermosensitivity (less than 1% yield at 39°C as compared to that of the wild-type virus) resulted from the change of the two U•A base pairs at positions 7 and 8 by either mirroring the two U•A base pairs into A•U pairs (virus Xm7–8) or the replacement into two U•G pairs [Xr7–8(U•G)] (Fig. 2D).

In addition, the significance of a C-A mismatch at position 6 was investigated by converting it into either an A-C mismatch (in virus Xm6) or a C•G base pair [Xr6(C•G)]. The viruses resulting from these mutations exhibited a wild-type phenotype (Table 1), indicating that the mismatch played no significant physiological role, at least under the conditions tested.

Thus, the primary sequence of the most distal base pair (U•A) of domain X and its position relative to other parts of the *ori*R appears to be an orientation-dependent recognition signal.

Identification of orientation-dependent recognition signals in domain Y

The adverse phenotypic effect of a base-pair insertion into position 5 of domain Y was compensated by a base-pair deletion at position 10 [virus Y+5(G•C)/Δ10] (Table 1), indicating that the rotation of the helix by 33° between these positions did not impair the *ori*R function. Also, mirroring the central, highly conserved portion (positions 7–9) of the Y domain through replacing $_{7339}$UAC$_{7341}$•$_{7370}$GUA$_{7372}$ by $_{7339}$AUG$_{7341}$•$_{7370}$CAU$_{7372}$ resulted in a virus (Ym7–9) with a wild-type-like phenotype (Table 1), suggesting that there are no strict primary structure requirements for this part of the Y domain. This was not the case, however, with distal positions 11 and 12, where the replacement of a C•G pair by a G•C pair resulted in a moderate and a strong temperature-sensitive phenotype, respectively (viruses Ym11 and Ym12; Fig. 2E).

The physiological importance of the specific spatial arrangement of the distal region of domain Y was also supported by the results obtained with the constructs in which an additional base pair was introduced just adjacent to its most distal base pair (i.e., distal to position 12). Indeed, the insertion of a G•C pair at this position [virus Y+12(G•C)] resulted in dead phenotype, and a temperature-sensitive virus [Y+12(C•G)] was generated upon a C•G pair insertion (Fig. 2F). The latter mutation resulted in two types of structural alterations: (1) the primary structure of the distal portion of domain Y was changed by the acquisition of the fourth consecutive C•G pair, and (2) a change occurred in the spatial position of the terminal C•G pair due to its rotation as well as lengthening of the domain. It was this altered spatial position of the terminal C•G pair that was responsible for the temperature-sensitive properties of the mutant. Indeed, the return of the ultimate base pair to its wild-type position upon combination of a C•G insertion distal to position 12 with a deletion of base pair 6 (virus YΔ6/+12(C•G) resulted in the restoration of the wild-type growth characteristics (Table 1).

Thus, both the primary structure of the two most distal base pairs of domain Y and their position relative to other parts of *ori*R appeared to play an important role in the function of this essential *cis*-acting replicative element.

DISCUSSION

The aim of the present study was to characterize some functionally significant structural features of a complex RNA control element, *ori*R, which is thought to be involved in the initiation of enterovirus negative RNA strand synthesis. This element is conserved among enteroviruses (Pilipenko et al., 1992b; Wang et al., 1999) and consists primarily of two hairpins, each containing two stacked coaxial helical elements (in the case of coxsackieviruses) that are joined to one another by the kissing interaction between their loops (Pilipenko et al., 1996; Melchers et al., 1997). The kissing interaction itself rather than its nucleotide sequence appears to be essential for the *ori*R function (Pilipenko et al., 1996; Melchers et al., 1997, Mirmomeni et al., 1997; Wang et al., 1999). Molecular dynamics calculations (H.J. Bruins Slot, E.V. Pilipenko, V.I. Agol & W.J.G. Melchers, unpubl.) suggest that this tertiary RNA interaction is relatively stable and thus may serve as a scaffold for the attached helical elements. The *ori*R function should involve its interactions with protein components of the replication machinery (reviewed in Agol et al., 1999), in which the helical elements are likely to be involved, as indicated by adverse biological effects of some of their modifications (Pierangeli et al., 1995; Rohll et al., 1995; this article). The recognition signals on the helical elements may involve specific nucleotide-sequence motifs and/or elements of secondary and tertiary structures, such as canonical and anomalous base pairs, bulges, etc. (Schuster et al., 1997; Uhlenbeck et al., 1997). We were primarily interested in ascertaining whether the spatial organization of domains (mutual orientation of recognizable signals) is of functional significance.

Strong evidence for the importance of a specifically required orientation of domain X relative to the orientation of domain Y was provided by the observations that mutations in one of them could be suppressed by mutations in the other. Indeed, the functional damage caused by a base-pair deletion in domain X could be suppressed by a base-pair deletion in domain Y, and the adverse effect of a base-pair insertion in domain Y was corrected by a base-pair insertion in domain X. We propose that certain elements of the two domains are simultaneously involved in the interaction with a ligand, most likely the multicomponent RNP composed of viral and host proteins. The relative rigidity of this ligand and the necessity of its concerted interaction with both domains creates constraints for the mutual orientation of X and Y helices. An alteration of the relative position of one helix requires an appropriate reply from the second. In this sense, domains X and Y are cross-talking. An understanding of the spatial interdependence of RNA moieties will be of great interest in understanding how RNA elements fold to interact with their ligands, and will contribute to our knowledge of the structural and biological function of RNA molecules and their interplay with the environment.

Phenotypic neutrality of the rotational and linear shifts of the portions of the X and Y helices located between the base-pair insertions and deletions in a given domain (e.g., viruses Y+5(G•C)/Δ10 and XΔ2/+8(U•A)),

demonstrated that these portions were hardly involved in the orientation-sensitive interactions with the ligands. The same could be said of the positions where mirroring or replacement did not affect the temperature dependence of viral reproduction. As evidenced by phenotypic consequences of the mutational alterations, the major recognizable determinants appeared to include the two most distal base pairs in each of the two helical domains. These determinants are the most likely candidates in the cross-talk phenomenon. The mechanism of their recognition is not known but appears to be different from the canonical interaction of a ligand with the grooves of a helix. This notion is based on the observation that a base-pair insertion distal to the terminal (twelfth) position of domain Y resulted in a replication defect, even though the structure and relative position of base pairs in the critical positions 11 and 12 remained unchanged. Thus, it seems that C•G pairs in positions 11 and 12 should, for some reason, be terminal in the domain. This property by itself, although essential, was insufficient. Indeed virus Y+12(C•G), retaining the wild-type structure and orientation of base-pairs at positions 11 and 12 and having two terminal C•G pairs, nevertheless exhibited a temperature-sensitive phenotype. This fact suggests that a combination of two features of domain Y are essential for efficient functioning of the *ori*R (containing an unchanged domain X): the two distal positions should be occupied by C•G pairs and the length of the helix should correspond to 12 bp. To rationalize the above observations, we suggest that assembly of the initiating RNP complex on the *ori*R involves recognition of the twelfth base pair of domain Y by a mechanism similar to intercalation of the aromatic moiety of an amino acid.

If the bottom base pairs of the two domains should be recognized simultaneously, a strict orientation of the twelfth base pair of domain Y and the eighth base pair of domain X relative to each other (and perhaps to other parts of the *ori*R as well) is required. Because the angle between helices X and Y remained constant in all of the mutants (because of the dominating kissing domain) and the rotational shifts caused by insertions/deletions comprised only a portion of the complete turn, the relative orientation of the bottom base pairs of the two domains could be approximated in the following way (Fig. 5). The relative positions of the pairs is represented by the vectors starting at C6 of pyrimidine and ending at C8 of purine; these vectors will be denoted as $\vec{X}$ and $\vec{Y}$, respectively. The relative orientation of these vectors could be depicted as the angle between $\vec{Y}$ and a virtual copy of $\vec{X}$ (named $\vec{X}'$) obtained by superimposing domains X and Y. In the wild-type virus, this angle was assumed to be equal to α (Fig. 5A). Rotational shifts due to a base-pair insertion/deletion should change it by $\sim 33^\circ$ clockwise or counterclockwise depending on the character of mutation and on the particular helix affected.

Remarkably, a clear correlation between the changes in this angle and the mutant phenotype could be seen. The two mutants with a wild-type phenotype, YΔ6 and X+1(C•G), possessed the angle $\gamma = \alpha - 33^\circ$ (Fig. 5C,D), whereas the two temperature-sensitive mutants, Y+5(C•G) and XΔ2, have different angles, w.t., YΔ6, and X+1(C•G), but mutually the same angle, namely $\beta = \alpha + 33^\circ$ (Fig. 5B,E). The introduction of a phenotypically suppressing mutation into the second domain (as in mutants Y+5(G•C)/X+1(C•G) and YΔ6/XΔ2) resulted in the restoration of the wild-type-like angle α (Fig. 5F,G). It might be concluded that the mutual orientations represented by angles α and γ were functionally equipotent. In other words, the mutual orientation of the bottom base pairs of domains X and Y represented by either of these angles was compatible with efficient binding of the putative ligand(s). In contrast, the *ori*R conformation represented by β resulted in impaired ligand binding as manifested by the temperature-sensitive phenotype of the mutants. An even more severe change in the angle, like $\xi = 360^\circ - \alpha$ in Ym12 (Fig. 5H), completely abrogated the functional ligand/*ori*R complex formation.

The twelfth base pair of domain Y and the eighth base pair of domain X are likely involved in stacking interactions with domains Z and S, respectively (Fig. 1). Therefore it cannot be rigorously ruled out that changes in the positions of the latter domains resulting from insertions/deletions in domain X and Y may contribute to the observed phenotypic effects. This possibility seems, however, not very likely because the complete deletion of the Z domain was not accompanied by any detectable phenotypic manifestations (W.J.G. Melchers, J.M.J.E. Bakkers & F.J.M. van Kuppeveld, unpubl. data).

Summing-up, cross-talking elements in the enterovirus *ori*R were discovered and characterized by using the genetic approach worked out in this study. This approach may prove to be useful for the identification of orientation-dependent *cis*-acting helical elements in other complex RNA structures.

MATERIALS AND METHODS

Cells and viruses

Virus propagation and viral RNA transfections were performed with Vero cells. The cells were grown in minimal essential medium (MEM) supplemented with 10% fetal bovine serum. After infection, cells were fed with MEM containing 3% serum and after transfection, MEM containing 10% serum was added. Virus titers were determined in eight replicates by titration decimal dilutions in 96-well microtiter plates (Melchers et al., 1997). $TCID_{50}$ values were calculated according to Reed and Muench (1938).

Site-directed mutagenesis

A full-length copy of DNA of coxsackie B3 virus (pCB3/T7) cloned behind a T7 RNA polymerase promoter was used

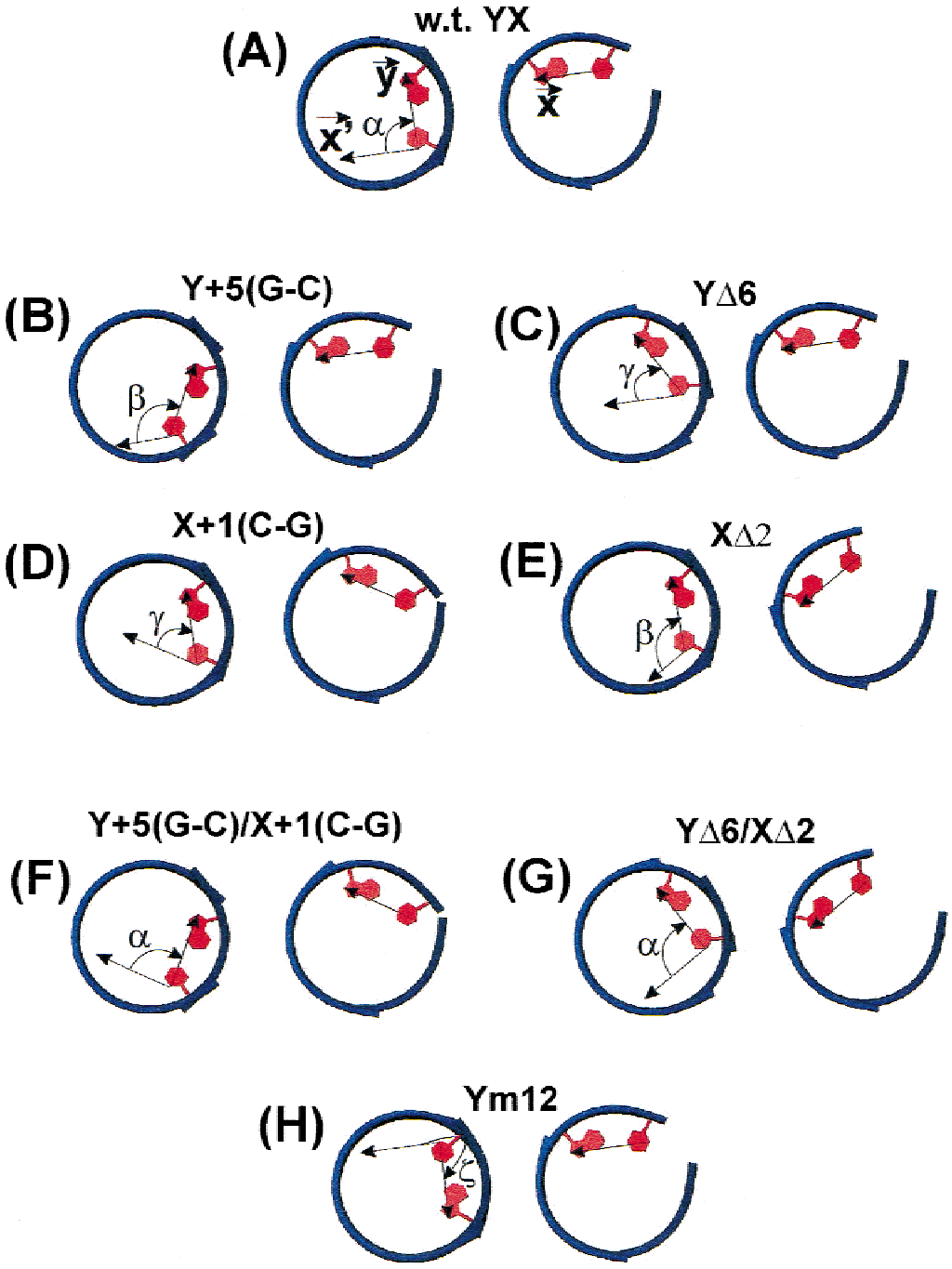

FIGURE 5. A schematic illustration of spatial relationship between the bottom base pairs of domains X (on the right) and Y (on the left) in the *ori*R of wild-type and mutant viruses. Each pair is shown in its own stem's coaxial projection from the kissing viewpoint. Vectors, $\vec{X}$ and $\vec{Y}$, are drawn starting from the C6 of pyrimidine and ending at the C8 of purine. A virtual copy of $\vec{X}$ ($\vec{X}'$) is shown also on the bottom base pair of Y. The angles between $\vec{X}'$ and $\vec{Y}$ are given in the clockwise direction. For other details, see text.

(Klump et al., 1990). For the oligonucleotide-directed mutagenesis, the 3′ UTR was cloned into phagemid pALTERtm-1 (Melchers et al., 1997) and mutations were introduced using the Altered Sites™ in vitro mutagenesis system (Promega) according to the recommendations of the manufacturer. Synthetic oligonucleotides (Biolegio, The Netherlands) were used to introduce site-specific mutations. The mutated fragments were cloned into pCB3/T7 and the nucleotide sequence of the mutant cDNAs was verified as described previously (Melchers et al., 1997).

Transfection of cells with RNA transcripts

pCB3/T7 plasmids were linearized by digestion with *Sal*I and transcribed in vitro by T7 RNA polymerase as described (Melchers et al., 1997). Vero cells were transfected in duplicates with 4 μg RNA using the DEAE-dextran method (Melchers et al., 1997). The cells were grown at 33 °C. The cells were incubated until CPE was complete. When no CPE was observed 5 days after transfection, the cell cultures were subjected to three cycles of freezing and thawing and 250 μL were subsequently passaged to fresh Vero cell monolayers. Upon CPE completion, the cultures were subjected to three cycles of freezing and thawing and the viruses were stored at −80 °C. When no CPE was observed 5 days after passage, the mutation was considered to be lethal.

Single-cycle growth analysis

Confluent Vero cell monolayers were infected with virus at a multiplicity of infection (MOI) of 1 $TCID_{50}$ per cell and grown at 33, 36, and 39 °C for 4, 6, and 8 h (Melchers et al., 1997). Viruses were released by three successive cycles of freezing and thawing and titrated at 36 °C.

Sequence analysis of mutant viruses

Viral RNA extraction, cDNA synthesis, and PCR amplification using a poly(T) primer and a primer located in the three-dimensional coding region (5′-GTTGTTTGACCCTCCCC GCG-3′) were performed as described (Melchers et al., 1997). The resulting 179-bp PCR products were purified from low-melting agarose and the nucleotide sequence of the 3′ UTR was determined as described (Melchers et al., 1997).

Chemical and enzymatic probing

RNA transcripts were generated and purified as described (Pilipenko et al., 1994). One microgram of full-length RNA transcripts was used for the probing. The conditions used to treat full-length copy RNA with dimethyl sulfate, RNase T1, cobra venom nuclease, *Bacillus cereus*, and Phy M nucleases have been described (Pilipenko et al., 1989a, 1994). To identify the sites where cleavages or modifications had occurred, 5′-end [^{32}P]-labeled oligonucleotides $(T)_{14}$CCC for pCB3-3′UTR/XΔ2 or $(T)_{14}$CCG for the other mutants (complementary to nt 7397–7413 of the virus RNA) were used as primers for cDNA synthesis.

ACKNOWLEDGMENTS

This research was supported by grants from the European Communities (INTAS/RFBR #01365.i96 and INTAS 97-10348), the Russian Foundation for Basic Research, and the Council for Chemical Sciences of the Netherlands Organization for Scientific Research (NWO-CW) grant 98008.

Received February 29, 2000; returned for revision April 6, 2000; revised manuscript received April 20, 2000

REFERENCES

Agol VI, Paul AV, Wimmer E. 1999. Paradoxes of the replication of picornaviral genomes. *Virus Res 62*:129–147.

Baeyens KJ, de Bondt HL, Pardi A, Holbrook SR. 1996. A curved RNA helix incorporating an internal loop with a G-A and A-A non-Watson–Crick base pairing. *Proc Natl Acad Sci USA 93*: 12851–12855.

Belsham GJ, Sonenberg N. 1996. RNA–protein interactions in regulation of picornavirus RNA translation. *Microbiol Rev 60*:499–511.

Deiman BALM, Pleij CWA. 1997. Pseudoknots: A vital feature in viral RNA. *Semin Virol 8*:166–175.

Fourmy D, Recht MI, Blanchard SC, Puglesi JD. 1996. Structure of the A-site of *Escherichia coli* 16S ribosomal RNA complexed with an aminoglycoside antibiotic. *Science 274*:1367–1371.

Frolov I, McBride MS, Rice CM. 1998. *Cis*-acting RNA elements required for replication of bovine viral diarrhea virus-hepatitis C virus 5′ nontranslated region chimeras. *RNA 4*:1418–1435.

Giege R. 1996. Interplay of tRNA-like structures from plant viral RNAs with partners of the translation and replication machineries. *Proc Natl Acad Sci USA 93*:12078–12081.

Gromeier M, Bossert B, Arita M, Nomoto A, Wimmer E. 1999. Dual stem loops within the poliovirus internal ribosomal entry site control neurovirulence. *J Virol 73*:958–964.

Gutell RR, Larsen N, Woese CR. 1994. Lessons from an evolving rRNA: 16S and 23S rRNA structures from a comparative perspective. *Microbiol Rev 58*:10–26.

Hellendoorn K, Verlaan PW, Pleij CW. 1997. A functional role for the conserved protonatable hairpins in the 5′ untranslated region of turnip yellow mosaic virus RNA. *J Virol 71*:8774–8779.

Hilbers CW, Michiels PJ, Heus HA. 1998. New developments in structure determination of pseudoknots. *Biopolymers 48*:137–153.

Hofacker IL, Fekete M, Flamm C, Huynen MA, Rauscher S, Stolorz PE, Stadler PF. 1998. Automatic detection of conserved RNA structure elements in complete RNA virus genomes. *Nucleic Acids Res 26*:3825–3836.

Hoffman MA, Palmenberg AC. 1996. Revertant analysis of J-K mutations in the encephalomyocarditis virus internal ribosomal entry site detects an altered leader protein. *J Virol 70*:6425–6430.

Holbrook SR, Cheong CJ, Tinoco I, Kim SH. 1991. Crystal structure of an RNA double helix incorporating a track of non-Watson–Crick base pairs. *Nature 353*:579–581.

Ishii T, Shiroki K, Iwai A, Nomoto A. 1999. Identification of a new element for RNA replication within the internal ribosome entry site of poliovirus RNA. *J Gen Virol 80*:917–920.

Jackson RJ, Kaminski A. 1995. Internal initiation of translation in eukaryotes: The picornavirus paradigm and beyond. *RNA 1*:985–1000.

Jacobson SJ, Konings DA, Sarnow P. 1993. Biochemical and genetic evidence for a pseudoknot structure at the 3′ terminus of the poliovirus RNA genome and its role in viral amplification. *J Virol 67*:2961–2971.

Jang SB, Hung LW, Chi YI, Holbrook EL, Carter RJ, Holbrook SR. 1998. Structure of an RNA internal loop consisting of tandem C-A+ base pairs. *Biochemistry 37*:11726–11731.

Kieft JS, Zhou K, Jubin R, Murray MG, Lau JY, Doudna JA 1999. The hepatitis C virus internal ribosome entry site adopts an ion-dependent tertiary fold. *J Mol Biol 292*:513–529.

Klovins J, Berzins V, van Duin J. 1998. A long-range interaction in Qβ RNA that bridges the thousand nucleotides between the M-site and the 3′ end is required for replication. *RNA 4*:948–957.

Klump WM, Bergmann I, Muller BC, Ameis D, Kandolf R. 1990. Complete nucleotide sequence of infectious coxsackievirus B3 cDNA: Two initial 5′ uridine residues are regained during plus-strand RNA synthesis. *J Virol 64*:1573–1583.

Kolk MH, van der Graaf M, Wijmenga SS, Pleij CW, Heus HA, Hilbers CW. 1998. NMR structure of a classical pseudoknot: Interplay of single- and double-stranded RNA. *Science 280*:434–438.

Kolykhalov AA, Feinstone SM, Rice CM. 1996. Identification of a highly conserved sequence element at the 3′ terminus of hepatitis C virus genome RNA. *J Virol 70*:3363–3371.

Le SY, Liu WM, Maizel JV Jr. 1998. Phylogenetic evidence for the improved RNA higher-order structure in internal ribosome entry sequences of HCV and pestiviruses. *Virus Genes 17*:279–295.

Lee K, Varma S, SantaLucia J Jr, Cunningham PR. 1997. In vivo

determination of RNA structure-function relationships: Analysis of the 790 loop in ribosomal RNA. *J Mol Biol 269*:732–743.
Lemon SM, Honda M. 1997. Internal ribosome entry sites within the RNA genomes of hepatitis C virus and other flaviviruses. *Semin Virol 8*:274–288.
Luck R, Steger G, Riesner D. 1996. Thermodynamic prediction of conserved secondary structure: Application to the RRE element of HIV, the tRNA-like element of CMV and the mRNA of prion protein. *J Mol Biol 258*:813–826.
Massire C, Jaeger L, Westhof E. 1998. Derivation of three-dimensional architecture of bacterial ribonuclease P RNAs from comparative sequence analysis. *J Mol Biol 279*:773–793.
Melchers WJ, Hoenderop JG, Bruins Slot HJ, Pleij CW, Pilipenko EV Agol VI, Galama JM. 1997. Kissing of the two predominant hairpin-loops in the coxsackie B virus 3′ UTR is the essential structural feature of the origin of replication required for (−) strand RNA synthesis. *J Virol 71*:686–696.
Mellits KH, Meredith JM, Rohll JB, Evans DJ, Almond JW. 1998. Binding of a cellular factor to the 3′ untranslated region of the RNA genomes of entero- and rhinoviruses plays a role in virus replication. *J Gen Virol 79*:1715–1723.
Mirmomeni MH, Hughes PJ, Stanway G. 1997. An RNA tertiary structure in the 3′ untranslated region of enteroviruses is necessary for efficient replication. *J Virol 71*:2363–2370.
Pierangeli A, Bucci M, Pagnotti P, Degener AM, Perez Bercoff R. 1995. Mutational analysis of the 3′-terminal extra-cistronic region of poliovirus RNA: Secondary structure is not the only requirement for minus strand RNA replication. *FEBS Lett 374*:327–332.
Pilipenko EV, Blinov VM, Chernov BK, Dmitrieva TM, Agol VI. 1989a. Conservation of the secondary structure elements of the 5′-untranslated region of cardio- and aphthovirus RNAs. *Nucleic Acids Res 17*:5701–5711.
Pilipenko EV, Blinov VM, Romanova LI, Sinyakov AN, Maslova SV, Agol VI. 1989b. Conserved structural domains in the 5′-untranslated region of picornaviral genomes: An analysis of the segment controlling translation and neurovirulence. *Virology 168*: 201–219.
Pilipenko EV, Gmyl AP, Maslova SV, Belov AP, Sinyakov AN, Huang M, Brown TDK, Agol VI. 1994. Starting window, a distinct element in the cap-independent internal initiation of translation on picornaviral RNA. *J Mol Biol 241*:398–414.
Pilipenko EV, Gmyl AP, Maslova SV, Khitrina EV, Agol VI. 1995. Attenuation of Theiler's murine encephalomyelitis virus by modifications of the oligopyrimidine/AUG tandem, a host-dependent translational cis element. *J Virol 69*:864–870.
Pilipenko EV, Gmyl AP, Maslova SV, Svitkin YV, Sinyakov AN, Agol VI. 1992a. Prokaryotic-like *cis* elements in the cap-independent internal initiation of translation on picornavirus RNA. *Cell 10*:119–131.
Pilipenko EV, Maslova SV, Sinyakov AN, Agol VI. 1992b. Towards identification of *cis*-acting elements involved in the replication of enterovirus and rhinovirus RNAs: A proposal for the existence of tRNA-like terminal structures. *Nucleic Acids Res 20*:1739–1745.
Pilipenko EV, Poperechny K, Maslova SV, Melchers WJ, Bruins Slot HJ, Agol VI. 1996. *Cis*-element, *ori*R, involved in the initiation of (−) strand poliovirus RNA: A quasi-globular multi-domain RNA structure maintained by tertiary ("kissing") interactions. *EMBO J 15*:5428–5436.
Reed LJ, Muench H. 1938. A simple method of estimating fifty per cent endpoints. *Am J Hyg 27*:493–497.
Robertson ME, Seamons RA, Belsham GJ. 1999. A selection system for functional internal ribosome entry site (IRES) elements: Analysis of the requirement for a conserved GNRA tetraloop in the encephalomyocarditis virus IRES. *RNA 5*:1167–1179.
Rohll JB, Moon DH, Evans DJ, Almond JW. 1995. The 3′ untranslated region of picornavirus RNA: Features required for efficient genome replication. *J Virol 69*:7835–7844.
Rust RC, Ochs K, Meyer K, Beck E, Niepmann M. 1999. Interaction of eukaryotic initiation factor eIF4B with the internal ribosome entry site of foot-and-mouth disease virus is independent of the polypyrimidine tract-binding protein. *J Virol 73*:6111–6113.
Schuster P, Stadler PF, Renner A. 1997. RNA structures and folding: From conventional to new issues in structure predictions. *Curr Opin Struct Biol 7*:229–235.
Smalle J, Kurepa J, Haegman M, Gielen J, van Montagu M, Straeten DV. 1998. The trihelix DNA-binding motif in higher plants is not restricted to the transcription factors GT-1 and GT-2. *Proc Natl Acad Sci USA 95*:3318–3322.
Springer MS, Douzery E. 1996. Secondary structure and patterns of evolution among mammalian mitochondrial 12S rRNA molecules. *J Mol Evol 43*:357–373.
Stewart SR, Semler BL. 1997. RNA-determinants of picornavirus cap-independent translation initiation. *Semin Virol 8*:242–255.
Stewart SR, Semler BL. 1998. RNA structure adjacent to the attenuation determinant in the 5′-non-coding region influences poliovirus viability. *Nucleic Acids Res 26*:5318–5326.
Tinoco I Jr, Bustamante C. 1999. How RNA folds. *J Mol Biol 293*: 271–281.
Todd SJ, Nguyen HC, Semler BL. 1995. RNA–protein interactions directed by the 3′ end of human rhinovirus genomic RNA. *J Virol 65*:3605–3614.
Uhlenbeck OC, Pardi A, Feigon J. 1997. RNA structures comes of age. *Cell 90*:833–840.
Wang J, Bakkers JM, Galama JM, Bruins Slot HJ, Pilipenko EV, Agol VI, Melchers WJ. 1999. Structural requirements of the higher order RNA kissing element in the enteroviral RNA. *Nucleic Acids Res 27*:485–490.
Wu M, Tinoco I Jr. 1998. RNA folding causes secondary structure rearrangement. *Proc Natl Acad Sci USA 95*:11555–11560.
Xiang W, Paul AV, Wimmer E. 1997. RNA signals in entero- and rhinovirus genome replication. *Semin Virol 8*:256–273.